



Published in final edited form as:

J Neurophysiol. 2008 May ; 99(5): . doi:10.1152/jn.01192.2007.

Differential Modulation of Neural Network and Pacemaker Activity Underlying Eupnea and Sigh-Breathing Activities

Andrew K. Tryba¹, Fernando Peña², Steven P. Lieske³, Jean-Charles Viemari^{4,6}, Muriel Thoby-Brisson⁵, and Jan-Marino Ramirez⁶

¹Department of Physiology, Medical College of Wisconsin, Milwaukee, Wisconsin

²Departamento de Farmacobiología, Cinvestav-Sede Sur, Mexico City, Federal District, Mexico

³Department of Psychiatry, University of California–San Francisco, San Francisco, California

⁴Laboratoire Plasticité et Physio-Pathologie de la Motricité, Centre National de la Recherche Scientifique Unité Mixte de Recherche 6196, Marseille

⁵Laboratoire de Neurobiologie Genetique et Integrative, Institut Alfred Fessard, Gif sur Yvette, France

⁶Department of Organismal Biology, The University of Chicago, Chicago, Illinois

Abstract

Many networks generate distinct rhythms with multiple frequency and amplitude characteristics. The respiratory network in the pre-Bötzinger complex (pre-Böt) generates both the low-frequency, large-amplitude sigh rhythm and a faster, smaller-amplitude eupneic rhythm. Could the same set of pacemakers generate both rhythms? Here we used an *in vitro* respiratory brain slice preparation. We describe a subset of synaptically isolated pacemakers that spontaneously generate two distinct bursting patterns. These two patterns resemble network activity including sigh-like bursts that occur at low frequencies and have large amplitudes and eupneic-like bursts with higher frequency and smaller amplitudes. Cholinergic neuromodulation altered the network and pacemaker bursting: fictive sigh frequency is increased dramatically, whereas fictive eupneic frequency is drastically lowered. The data suggest that timing and amplitude characteristics of fictive eupneic and sigh rhythms are set by the same set of pacemakers that are tuned by changes in the neuromodulatory state.

INTRODUCTION

Many neuronal networks including those involved in sleep, olfaction, learning, and locomotion generate multiple, context-dependent rhythms (Csicsvari et al. 2003; Kay 2003; Steriade et al. 1993a; Tryba and Ritzmann 2000). Respiratory rhythms are critical to life and several forms of rhythmic activities are generated by the medullary respiratory neural network. Under normal conditions, breathing includes eupnea (“normal respiration”), which transforms into gasping during severe hypoxia (Lieske et al. 2000). During normal breathing, the low-frequency sigh rhythm is superimposed on eupneic activity and includes larger inspiratory efforts. Each sigh is followed by postsigh apnea and phase resetting of the eupneic rhythm.

Sighing is a normal component of breathing and serves to reopen collapsed alveoli (Issa and Porostocky 1993); sighs are thought to trigger arousal, failure of which may contribute to sudden infant death syndrome (SIDS) (Franco et al. 2003). Despite its clinical relevance, the mechanisms underlying sigh generation remain largely unknown (Lieske and Ramirez 2006a,b; Lieske et al. 2000).

A better understanding of the mechanisms underlying eupnea and sighs is facilitated by the medullary slice preparation of mice that contains a critical portion of the respiratory neural network—the pre-Bötzinger complex (pre-Böt)—that simultaneously generates fictive eupneic and sigh activities. Stereotactic mapping of the population activity recorded at the slice surface revealed extensive spatial overlap in the network active during eupnea and sighs, which suggested that the same network generates different forms of breathing (Lieske et al. 2000).

Patch-clamp data indicate most pre-Böt inspiratory neurons produce a burst of action potentials during both fictive eupnea and sighs (Lieske et al. 2000). Thus previously described inspiratory neurons typically contribute to both fictive eupneic and sigh activity (Lieske et al. 2000). However, detailed synaptic analysis revealed distinct synaptic properties underlie eupneic and sigh rhythm generation (Lieske and Ramirez 2006a,b) and suggest the possibility that distinct populations of inspiratory neurons underlie sigh rhythm generation. These data pose a very interesting puzzle that is relevant to many rhythmic neural networks: What types of cellular mechanisms allow largely overlapping networks to generate two superimposed and interacting rhythms?

The identification of nonpacemaking, “sigh-only” neurons in the present study is consistent with the hypothesis that distinct sigh-specific neuron populations exist. However, this finding does not resolve the core question: How do two largely overlapping neuronal networks generate two distinct inspiratory rhythms? Here, we describe the unexpected finding that some synaptically isolated pacemaker neurons generate two types of bursts, each having distinct amplitude and timing characteristics: fast, low-amplitude bursts are interrupted by low-frequency, large-amplitude bursts. Oxotremorine, a muscarinic agonist, transforms the timing characteristics of this subset of respiratory pacemakers by increasing the frequency of large-amplitude bursts while simultaneously decreasing low-amplitude burst frequency. The network responds with similar timing changes: the very low frequency (and large-amplitude) fictive sighs increased their frequency dramatically, whereas the ordinarily much faster (and lower-amplitude) fictive eupneic rhythm shows the opposite effect, slowing considerably and, in some cases, stopping altogether. Thus the allegiance to these rhythms depends on the neuromodulatory state that alters pacemaker and network properties.

METHODS

All experiments conformed to the guiding principles for the care and use of animals approved by the National Institutes of Health and the Animal Care and Use Committees at the Medical College of Wisconsin and The University of Chicago (experimental performance sites).

Medullary brain slice and pre-Bötzinger complex island preparation

All experiments used the transverse, rhythmic 600- to 650- μm -thick medullary brain slice obtained from 1- to 13-day-old CD-1 outbred mice (Charles River Laboratories, Wilmington, MA) (Thoby-Brisson and Ramirez 2001). CD-1 mice were deeply anesthetized with ether (delivered by inhalation) and quickly decapitated at the C3/C4 spinal level (Thoby-Brisson and Ramirez 2001). The brain stem was dissected in ice-cold artificial

cerebral spinal fluid (ACSF) that was equilibrated with carbogen (95% O₂-5% CO₂, pH 7.4). Rhythmic slice preparations containing the pre-Bötzinger complex (pre-Böt) were obtained by slicing the medulla using a microslicer (VT1000S; Leica, Nussloch, Germany). Slices were submerged in a recording chamber (6 ml) under circulating ACSF (30°C; flow rate 17 ml/min, total circulating volume = 200 ml).

ACSF contained (in mM): 118 NaCl, 3 KCl, 1.5 CaCl₂, 1 MgCl₂·6H₂O, 25 NaHCO₃, 1 NaH₂PO₄, and 30 D-glucose, equilibrated with carbogen (95% O₂-5% CO₂, pH 7.4). All ACSF chemicals were obtained from Sigma (St. Louis, MO). Extracellular KCl was elevated from 3 to 8 mM over a span of 30 min before commencing recordings, to maintain rhythmic population activity (Tryba et al. 2003). Note that raising ACSF external potassium ([K⁺]_o) does not artificially introduce pacemaker bursting properties; pacemakers show similar bursting properties in 3 versus 8 mM [K⁺]_o ACSF (Tryba et al. 2003). Further, it should be noted that [K⁺]_o changes on a breath-by-breath basis and changes in [K⁺]_o do not obviously alter the form of respiratory activity generated because both eupneic and gasping activities can be recorded in hypokalemic and hyperkalemic conditions in situ (St-John et al. 2005). Bath temperature was monitored and maintained at 30 ± 0.7°C using a Warner Instrument (Hamden, CT) TC-344B temperature regulator with an in-line solution heater (SH-27B); bath temperature at various locations within the bath was uniform. The ventral respiratory group (VRG)-island preparation (Johnson et al. 2001) was made by taking a brainslice preparation and cutting a wedge-shaped piece of tissue containing the pre-Böt complex out of the transverse brainslice using a sharp razor blade.

Electrophysiology: population activity and identification of inspiratory neurons

Extracellular recordings were obtained with glass suction electrodes positioned on the slice surface in the VRG near or on top of the pre-Böt (Fig. 1, A and B) (Tryba et al. 2003). The VRG population bursting is dominated by inspiratory neurons such that integrated VRG (\int VRG) activity is in-phase with integrated XII (\int XII) activity (Tryba et al. 2006). Thus VRG population bursts serve as a marker of fictive inspiration (Tryba et al. 2006). This population activity was rectified and integrated and the data were digitized with a Digidata acquisition system (Molecular Devices, Sunnyvale, CA), stored on an IBM-compatible PC using Axoscope 10 (Molecular Devices) software, and analyzed off-line using Igor Pro (WaveMetrics, Lake Oswego, OR). The \int VRG population burst amplitude was measured as baseline to peak height, whereas frequency was calculated based on the burst intervals. To minimize the potential influence of baseline fluctuations and differences in burst peak trajectories, the \int VRG burst duration was calculated as the duration of the burst at half-maximal burst amplitude.

Intracellular patch-clamp recordings were obtained with a Multi-Clamp 700B amplifier (Molecular Devices), applying the blind-patch technique to VRG neurons in 600- to 650- μ m brain stem slice preparations (Thoby-Brisson and Ramirez 2001). Patch electrodes were manufactured from filamented borosilicate glass tubes (Clark G150F-4; Warner Instruments) and filled with an intracellular solution containing (in mM): 140 K-gluconic acid, 1 CaCl₂·6H₂O, 10 EGTA, 2 MgCl₂·6H₂O, 4 Na₂ATP, and 10 HEPES.

Only inspiratory VRG neurons active in-phase with the \int VRG population burst were recorded in this study. The discharge pattern of each cell type was first identified in the cell-attached mode and remained similar in whole cell configuration (Peña et al. 2004). Experiments were then performed in the whole cell patch-clamp mode. The membrane voltage (V_m) values were corrected for the liquid junction potential as calculated using pClamp 10 software (Molecular Devices). In current clamp, neurons were isolated from ionotropic chemical synaptic input using a mixture of glutamatergic, GABAergic, and glycinergic antagonists. These drugs were bath applied at the final concentrations of: 20 μ M

6-cyano-7-nitroquinoxaline-2,3-dione (CNQX; Tocris Bioscience, Ellisville, MO), 10 μM (*RS*)-3-(2-carboxypiperazin-4-yl)-propyl-1-phosphonic acid [(*RS*)-CPP, or CPP; Tocris], 1 μM strychnine (Sigma), and 20 μM bicuculline-free base (Sigma). Note that unlike bicuculline methiodide, the bicuculline-free base derivative is a specific γ -aminobutyric acid (GABA)-receptor antagonist that does not block apamin-sensitive Ca^{2+} -activated K^{+} currents (Debarbieux et al. 1998; Johnson and Seutin 1997).

A subset of neurons, considered pacemakers, continued to exhibit voltage-dependent intrinsic bursting properties following blockade of ionotropic glutamate, GABA, and glycinergic receptors. These pacemakers met several criteria before being classified as inspiratory pacemaker neurons; the criteria used here are provided in detail elsewhere (Thoby-Brisson and Ramirez 2001; Tryba et al. 2003). Briefly, after isolation of the neuron from chemical synaptic input with bath-applied CNQX, CPP, strychnine, and bicuculline, pacemakers continued to burst in the absence of VRG population bursts. Second, isolated pacemakers exhibited voltage-dependent bursting properties. That is, brief depolarizing current injection could evoke a burst or hyperpolarizing current could terminate an ongoing burst; either of these reset the ongoing pacemaker bursting rhythm. Finally, depolarizing current injection increased, and injected hyperpolarizing current decreased, the bursting frequency. After synaptic isolation with CNQX, CPP, bicuculline, and strychnine, in some cases, cadmium (Cd^{2+}), a broad-spectrum calcium channel blocker, was used as a tool to discriminate between pacemaker neurons whose endogenous bursting mechanism is dependent on calcium versus sodium. Synaptically isolated pacemakers that continue to burst in the presence of voltage-gated calcium channel blockade with 200 μM Cd^{2+} are described as Cd^{2+} -insensitive (CI) pacemakers (Thoby-Brisson and Ramirez 2001) and are typically riluzole sensitive (Peña et al. 2004). Isolated pacemakers that cease bursting in Cd^{2+} are Cd^{2+} -sensitive (CS) pacemakers (Thoby-Brisson and Ramirez 2001) and have been shown to be FFA sensitive (Peña et al. 2004). Note that 200 μM Cd^{2+} ensures blockade of voltage-activated calcium currents in VRG neurons (Elsen and Ramirez 1997). Thus following bath application of 200 μM Cd^{2+} calcium-dependent chemical synaptic transmission should be blocked.

We describe here a new subset of pacemakers that produce two distinct kinds of bursts, characterized as eupneic-like versus sigh-like (see RESULTS). These two burst types were qualitatively quite distinct and, in light of the small number of sigh-like bursts, were initially identified by hand. The criteria used to identify sigh-like bursts included 1) a larger-amplitude inspiratory drive; 2) lower frequency; 3) longer duration than that of eupneic-like bursts; and 4) longer postburst quiescent period (corresponding to the postsigh apnea at the population level). To verify that the two bursts are distinct, we made statistical comparisons of the eupneic-like and sigh-like bursts so identified (presented in RESULTS).

Working heart– brain stem preparation

We used the in situ perfused working heart– brain stem preparation (Paton 1996) following methods previously described by Ramirez and Viemari (Elsen and Ramirez 2005). For these preparations, CD1 mice (P21 and older) were deeply anesthetized with ether and the brain was transected at the precollicular level. The rostral part of the transaction, including the pons, was removed (Elsen and Ramirez 2005). A second transection was performed subdiaphragmatically and the thorax–brain stem preparation was submerged in ice-cold ACSF (same ACSF as described for slices preparation) gassed with carbogen (95% O_2 -5% CO_2). The preparation was transferred to a recording chamber where brain tissue rostral to the medulla was removed under a binocular dissecting microscope. A cut was made just caudal to the facial nerve (Ramirez and Viemari 2005) and the pons was removed from the preparation. The abdominal aorta was cannulated for retrograde perfusion with ACSF

containing 3 mM K⁺. Oxotremorine (Tocris Cookson, Ballwin, MO) was added to the perfusate at a concentration of 10 μM. Inspiratory motor output was monitored by placing an extracellular suction electrode on the phrenic nerve. The signals were amplified 2,000-fold, filtered (low-pass 1.5 kHz; high-pass 250 Hz), rectified, and integrated using an electronic filter (time constant of 30–50 ms). All recordings were stored on a personal computer using Axoscope 10 (Molecular Devices) software and analyzed off-line using analysis software written with Igor Pro (WaveMetrics).

RESULTS

Fictive sighs in vitro

As first described by Lieske et al. (2000), fictive sighs occur periodically in the in vitro transverse medullary slice preparation from mice, containing the VRG (Fig. 1, *A* and *B*). Each fictive sigh burst is biphasic in shape, larger in amplitude ($P = 0.001$), longer in duration ($P = 0.001$), and occurs at a lower frequency ($P = 0.001$) than isolated eupneic bursts (Fig. 1, *C* and *D*, paired *t*-tests of mean values from $n = 15$ preparations, including $n = 1,840$ fictive eupneic and $n = 61$ sigh bursts). Note that the biphasic shape of sigh bursts typically arises as the result of being triggered by eupneic bursts, giving rise to a longer inspiratory duration than isolated fictive eupneic bursts (Fig. 1*C*). Our analysis included between $n = 3$ and $n = 6$ fictive sigh bursts per slice preparation (average $n = 4$ fictive sigh bursts/preparation).

We also verified that fictive sigh amplitude, duration, and frequency can be distinguished from those variables in eupneic bursts, by performing an unpaired *t*-test for each condition and preparation. In each case, there was a significant difference in eupneic and sigh amplitude ($P = 0.001$, unpaired *t*-test), duration ($P = 0.005$, Mann–Whitney rank-sum test), and frequency ($P = 0.005$, Mann–Whitney rank-sum test).

Sighs are followed by a brief pause in the eupneic rhythm, the so-called postsigh apnea (Cherniack et al. 1981). A fictive apnea is also observed after in vitro sighing activity (Fig. 1, *A* and *B*) (Lieske et al. 2000). Thus the above-cited characteristics of fictive sigh-like bursts recorded in vitro (i.e., biphasic shape, longer duration, larger-amplitude inspiratory activity, slower frequency, and postsigh apnea) are consistent with the definition of sighs in vivo (Cherniack et al. 1981; Glogowska et al. 1972; Orem and Trotter 1993; Takeda and Matsumoto 1998). As is the case for fictive sigh bursts in vitro (Fig. 1, *A* and *C*), the biphasic shape of the sigh, in vivo, has been interpreted as consisting of an initial phase that is identical to normal eupneic breathing activity but includes a later high-amplitude phase that is coupled to, and triggered by, the initial phase.

Both fictive sighs and fictive eupneic activity were also recorded in VRG-island preparations ($n = 4$; Fig. 1, *E* and *F*), obtained by trimming away tissue outside the ventral respiratory group (VRG) (Johnson et al. 2001), suggesting that the neurons responsible for generating both rhythms are contained within this region. Sighs generated in VRG islands (Fig. 1, *E–G*) were qualitatively similar to those recorded from the brain stem slice preparation because both included fictive eupneic activity and slower, eupneic-triggered fictive sighs (Fig. 1, *A–F*) (Lieske et al. 2000).

We additionally quantitatively analyzed fictive sigh bursts in the VRG islands (Fig. 1, *G* and *H*). Fictive sigh bursts in the VRG islands were also biphasic in shape, larger in amplitude ($P = 0.001$), longer in duration ($P = 0.001$), and occur at a lower frequency ($P = 0.001$) than isolated eupneic bursts (Fig. 1, *G* and *H*; paired *t*-tests of mean values from $n = 4$ VRG-island preparations, including $n = 460$ fictive eupneic and $n = 24$ sigh bursts). Our analysis

included between $n = 3$ and $n = 12$ fictive sigh bursts per slice preparation (average $n = 6$ fictive sigh bursts/preparation; Fig. 1H).

To additionally verify that in the VRG-island preparation, fictive sigh amplitude, duration, and frequency can be distinguished from those variables in fictive eupneic bursts, we performed an unpaired *t*-test for each condition and preparation. In each case, there was a significant difference in eupneic and sigh amplitude ($P = 0.001$, Mann–Whitney rank-sum test), duration ($P = 0.001$, Mann–Whitney rank-sum test), and frequency ($P = 0.001$, Mann–Whitney rank-sum test).

As was the case in the slice preparation (Lieske and Ramirez 2006b; Lieske et al. 2000) fictive sighs generated by the VRG island could be selectively abolished with $4 \mu\text{M}$ cadmium (Fig. 1E, $n = 3/3$ preparations). These data indicate the isolated VRG contains sufficient neuronal tissue to generate fictive sighs and also indicate that bilateral synchronization between pre-Böt nuclei is not required to generate sighs.

Fictive sigh-only neurons

We found a previously undescribed class of inspiratory neurons that are activated only during sigh bursts and call these “sigh-only” neurons (Fig. 2; $n = 26$ sigh-only cells recorded in $n = 26$ additional slice preparations; these preparations were different from the slices used in the preceding population studies). Here, we refer to these neurons as “sigh-only” because they are active during sighs, but not eupnea. However, this does not rule out the possibility of their participation in other respiratory activities.

Sigh-only neurons represent a minority of inspiratory neurons recorded in current clamp because most inspiratory neurons appear to burst during both fictive eupneic inspiratory activity and fictive sighs (Lieske et al. 2000). For example, in a subset of all our inspiratory neuron recordings, a sample including $n = 265$ inspiratory neurons, we found 4.9% ($n = 13$) were sigh-only neurons. Sigh-only neurons had varied firing patterns, some spiking sporadically between sighs (Fig. 2A, *i* and *ii*, $n = 18$), others tonically active but inhibited during eupnea (Fig. 2Bi, $n = 8$), yet all were bursting during fictive sighs (Fig. 2, $n = 26$).

A concern when using the whole cell current-clamp recording technique is that the technique may alter the intracellular milieu and in turn alter neural firing patterns. Thus prior to rupturing the cell-attached membrane seal, we identified the discharge pattern of sigh-only neurons in the cell-attached mode and found that it remained similar in whole cell configuration, such that “sigh-only” neurons exhibited a burst of action potentials coincident only with the population sigh burst, but not during fictive eupneic activity (Fig. 2A, *i* and *ii*).

To test whether sigh-only neurons required synaptic input to rhythmically trigger sigh bursts, we bath-applied CNQX ($20 \mu\text{M}$), CPP ($10 \mu\text{M}$), bicuculline ($20 \mu\text{M}$), and strychnine ($1 \mu\text{M}$). These synaptic antagonists eliminated fictive sigh-only cell bursts as well as fictive eupnea and sigh bursts at the population level (Tryba et al. 2003). None of the sigh-only neurons tested was an endogenous sigh pacemaker capable of generating intrinsic rhythmic activity following blockade of glutamatergic synaptic input ($n = 7$) or following combined blockade of glutamatergic and inhibitory synaptic transmission ($n = 6$) (Fig. 2B, *i* and *ii*).

Muscarinic activation suppresses fictive eupneic activity and enhances sighs

Neuromodulators can play a major role in determining respiratory rhythmogenesis (Peña and Ramirez 2002, 2004; Tryba et al. 2006; Viemari et al. 2005). Here, we found that application of the muscarinic agonist oxotremorine ($20 \mu\text{M}$) to the slice preparation markedly decreased, or abolished, fictive eupneic activity and increased fictive sigh-burst frequency (Fig. 3, A–D; Fig. 4A, $n = 10$ slice preparations). In six additional preparations,

bath application of a lower concentration of oxotremorine (10 μM) had similar effects, by increasing the number of fictive sighs from $n = 25$ (control, >10 min) to $n = 120$ (in oxotremorine, 10 min) and decreasing the number of fictive eupneic bursts from $n = 421$ (control, 10 min) to $n = 162$ (in oxotremorine, 10 min) (Fig. 4B).

Bath application of the M3-preferring muscarinic acetylcholine receptor (mAChR) antagonist 4-diphenylacetoxy-*N*-methylpiperidine-methiodide (4-DAMP, 1 μM), 10 min prior to applying 10 μM oxotremorine, blocked the effect of oxotremorine application alone, suggesting that oxotremorine application suppresses fictive eupnea and enhances sighs by activating M3 mAChRs (Fig. 4, B and C).

We tested whether oxotremorine also suppresses fictive eupnea and enhances fictive sighing frequency in a more intact network, using the in situ working heart–brain stem preparation (Paton 1996) (Fig. 4, D–F). When oxotremorine (10 μM) is perfused in the working heart–brain stem preparation, fictive eupneic frequency is suppressed ($P = 0.02$; Student's paired *t*-test), whereas fictive sigh bursts increase ($P = 0.029$) (Fig. 4D, $n = 4$ preparations, Student's paired *t*-test). As in vitro (Fig. 1C), fictive in situ eupneic \int phrenic bursts are distinct from biphasic sigh bursts because the latter have a larger amplitude ($P < 0.001$), longer duration ($P < 0.001$), and occur at a lower frequency ($P < 0.001$) (Fig. 4, E and F, $n = 5$ preparations, Student's paired *t*-test).

Pacemakers with endogenous sigh-like bursting properties

Having established that neurons contained within the VRG suffice to generate fictive sighs, in additional experiments, this area was targeted for extracellular and whole cell current-clamp recordings in the medullary slice preparation to determine how fictive sighs are generated. Two basic types of inspiratory pacemaker neurons were previously described that generate endogenous, voltage-dependent bursting after being synaptically isolated from ionotropic glutamatergic input (Peña et al. 2004; Thoby-Brisson and Ramirez 2001). The bursting mechanism of one type of pacemaker is sensitive to cadmium and flufenamic acid (FFA); the other type is insensitive to cadmium and FFA but sensitive to riluzole.

All inspiratory pacemaker neurons that were previously described burst during both eupnea and sighs when embedded in the respiratory network (Lieske et al. 2000). We refer to these cells as pacemakers because, following isolation from glutamatergic synaptic input with CNQX, CPP, and isolation from inhibitory transmission with bicuculline and strychnine, they exhibited endogenous, voltage-dependent pacemaker properties (Fig. 5, A and B) (Peña et al. 2004; Thoby-Brisson and Ramirez 2001). Most pacemakers do not continue to generate fictive sigh-like bursts following synaptic isolation (Fig. 5B), but retain their voltage-dependent bursting properties (Fig. 5C) (Lieske et al. 2000).

After isolation from chemical synaptic transmission, we found a subset of pacemaker neurons that differ from those previously described in that they continued to generate two types of bursts, at two different frequencies ($n = 5$), including a fictive “eupneic-like” burst and a fictive “sigh-like” burst. It must be emphasized that the terms “eupneic-like” and “sigh-like” are used here descriptively because the burst pattern parallels the network bursting fictive eupneic (fast-frequency, smaller-amplitude bursts) and sigh activities (lower-frequency, large-amplitude bursts). Fictive eupneic-like pacemaker bursts occur at a higher frequency ($P < 0.03$, paired *t*-test) and are shorter in duration ($P = 0.041$, paired *t*-test) than the lower-frequency sigh-like bursts; sigh-like bursts are also followed by a delay before eupneic-like bursts resume (Fig. 6A).

These cells are considered pacemaker neurons by virtue of the persistence of voltage-dependent rhythmic bursting following synaptic isolation with CNQX, CPP, bicuculline, and

strychnine (Fig. 6A). In addition, all five of these cells remained rhythmic in cadmium (Fig. 6B, $n = 4$) or FFA (Fig. 7, $n = 1$), indicating that they constitute a subset of the type of pacemaker referred to as CI pacemakers (Peña et al. 2004; Thoby-Brisson and Ramirez 2001).

The absence of VRG population bursting after blocking synaptic transmission raises the question as to whether the two burst types observed in these cells bear any relation to fictive eupnea and sighs at the population level. To address this question, we relied on the differential effect of oxotremorine application, which in the intact network increased fictive sigh network frequency while decreasing fictive eupneic frequency (Fig. 4, A and D). When bath applied to these dual-bursting pacemakers, in synaptic isolation, oxotremorine (20 μM) transformed their bursting from generating both fictive eupneic-like and sigh-like bursts, to preferentially generating sigh-like bursts at an increased frequency (Fig. 7A). On average, the frequency of fictive sigh-like bursts increased from 0.027 (± 0.0056 SD) to 0.089 Hz (± 0.037 SD; $P = 0.026$, paired t -test of means). This analysis included 29 sigh-like bursts (average of 5.8 sigh bursts per neuron) before adding oxotremorine and $n = 76$ fictive sigh-like bursts after adding oxotremorine (average of 15.2 sigh-like bursts per neuron) over the same duration ($P = 0.02$, paired t -test of means). This shift was accompanied by a relative hyperpolarization during the interburst interval and a cessation of interburst spiking (Fig. 7A).

In addition to the five pacemakers characterized earlier, there were an additional two pacemakers (rhythmic in synaptic isolation) that produced bursts that met the criteria that we have used here to screen for sigh-like bursts (larger-amplitude inspiratory drive, lower frequency, longer duration, and longer postburst quiescent period). These two cells were also cadmium insensitive, but differed from those characterized earlier in that the shape of the putative sigh-like bursts was less qualitatively distinct from the eupneic-like bursts and in that they were rendered quiescent after application of 20 μM oxotremorine (Fig. 7B).

Postsigh apnea

Following a sigh, a brief postsigh apnea occurs before eupnea resumes (Fig. 8A). At the network level, the postsigh apnea is significantly reduced by blocking N-type calcium channels, an effect hypothesized to be due to reduction of a Ca^{2+} -activated K^+ [$\text{IK}_{(\text{Ca}^{2+})}$] current (Lieske and Ramirez 2006b). The delay in fictive eupnea [that had a mean 2.14 ± 0.52 (SD) cycles, $n = 39$ sighs], following a fictive sigh burst, could also (in part) result from synaptic inhibition of inspiratory neurons immediately following a sigh. Along these lines, blockade of glycinergic and GABAergic transmission reduced the duration of the postsigh apnea ($n = 23$ sighs, $P = 0.004$, paired t -test of means), but it still occurred and delayed eupnea by an average of 1.73 cycles (± 0.50 SD, $n = 10$ preparations, Fig. 8B). Because blocking synaptic inhibition did not eliminate the postsigh apnea, these experiments suggest that the postsigh apnea may result in part from an intrinsic membrane property of inspiratory neurons.

DISCUSSION

The respiratory neural network simultaneously generates two distinct rhythms: a faster, lower-amplitude rhythm and slower, larger-amplitude rhythm, corresponding to fictive eupnea and fictive sighs, respectively. The muscarinic agonist oxotremorine alters the timing of these rhythms: fictive sighs speed up, whereas fictive eupneic activity slows considerably. This network effect was likely due to M3-mAChR activation because it was antagonized by 4-DAMP.

Embedded in the network are pacemakers that can generate two distinct burst patterns within the same neuron (or between two such neurons coupled by gap junctions). These burst patterns include both fast low-amplitude and slow large-amplitude bursts. In the presence of oxotremorine the timing of these intracellularly generated bursts was altered in a manner similar to the entire network. Large-amplitude bursts accelerate, whereas low-amplitude bursts are slowed. There were, however, two pacemakers, with dual-burst patterns that were silenced in oxotremorine. It is unclear whether they are more appropriately considered to be a different subclass of dual-bursting pacemakers or single-bursting pacemakers with a highly variable bursting pattern.

The ability to generate multiple behavioral rhythms is a common property of many networks, including the respiratory network. The neocortex, for example, generates rhythms covering diverse frequency bands that can be associated with different brain states (Buzsáki and Draguhn 2004; Chrobak and Buzsáki 1994; Steriade 2006; Steriade et al. 1993a). However, unlike fictive eupnea and sigh bursts, these neocortical rhythms are not known to occur concurrently. Similar phenomena exist in the olfactory bulb (Kay 2003; Tabor et al. 2004). Perhaps a more relevant example of a network capable of generating multiple rhythms is the stomatogastric ganglion (STG) of crustaceans, where neurons exist that participate in both the gastric and pyloric rhythms (Prinz et al. 2004).

Analysis of the STG led to important insights into the cellular mechanisms that underlie the generation of multiple rhythms (Prinz et al. 2004). STG neurons can switch between rhythms depending on neuromodulatory influence (Dickinson 1995; Goaillard et al. 2004; Hooper and Moulins 1989; Meyrand et al. 1991; Weimann and Marder 1994), which is similar to the oxotremorine response of respiratory neurons described here. Like mammalian respiratory neurons, many STG neurons simultaneously express multiple network rhythms (Meyrand et al. 1991; Weimann and Marder 1994). In doing so, STG neurons are essentially “multiplexing” by expressing two ongoing rhythms reflecting influences of different, yet overlapping, networks (Heinzel and Selverston 1988; Thuma and Hooper 2002; Weimann et al. 1991) that are characterized by distinct local synaptic connections (Bartos and Nusbaum 1997; Clemens et al. 1998) and synapses derived from upstream neuronal networks (Bartos and Nusbaum 1997; Marder et al. 1998; Wood et al. 2004). The situation is reminiscent of the respiratory network in that distinct synaptic properties may also govern eupneic and sigh rhythm generation (Lieske and Ramirez 2006a,b) that can be modulated by upstream neuronal networks (Alheid et al. 2004). However, rhythmic multiplicity in the STG is lost on synaptic isolation of these neurons. For example, the isolated “AB” neuron functions as a timing oscillator of the faster pyloric rhythm, but not the gastric rhythm (Weimann and Marder 1994). The period of the gastric rhythm is an emergent property that depends on many time constants in many different neurons (Weimann and Marder 1994).

Within the respiratory network we (and others) described two types of pacemaker neurons (Del Negro et al. 2005; Peña et al. 2004; Thoby-Brisson and Ramirez 2001), the timing of which resembles the eupneic rhythm more closely than the very slow sigh rhythm. Since these pacemakers express a wide range of timing parameters, it is conceivable that the period of the eupneic rhythm is an emergent property dependent on intrinsic time constants in many neurons and their synaptic interactions (Feldman and Del Negro 2006). Here we report pacemakers that simultaneously generated bursts with properties resembling those of the slow and large-amplitude sigh rhythm and fast and small eupneic rhythm. To the best of our knowledge neurons with intrinsic pyloric and gastric-like bursting properties have not previously been described in the STG. The overlap between the two stomatogastric rhythms is generated entirely by synaptic interactions.

It may seem surprising that in the mammalian respiratory network, fictive eupneic and sigh rhythms are apparently also reflected in single-neuron activity. However, the respiratory network may not be an exception. Single neocortical neurons can intrinsically generate beta activity that transforms into gamma oscillations following membrane depolarization (Gray and McCormick 1996; Steriade et al. 1993b). This transformation is reminiscent of global EEG changes that fluctuate between distinct rhythmic states during different mental activities (Steriade 2006; Steriade et al. 1993b). Similar to the respiratory network, the expression of two neocortical rhythms in the same neuron does not mean that both rhythms are associated with the same network mechanisms. Accordingly, distinct synaptic mechanisms shape both gamma and beta activity (Steriade 2006). Eupnea and sighs are also shaped by distinct synaptic network mechanisms (Lieske and Ramirez 2006a,b). Thus irrespective of the finding that single neurons can generate two types of rhythms and amplitude parameters, network rhythms occurring in a variety of rhythmic frequencies and patterns are typically the result of different electrophysiological characteristics and distinct connectivity features. However, this raises the important question: Is the similarity between the electrophysiological properties of single neurons and the network output just an epiphenomenon?

Although some suggest that respiratory pacemakers play critical roles in respiratory rhythmogenesis (Feldman and Smith 1989; Peña et al. 2004; Tryba et al. 2006), others suggest that eupneic rhythmogenesis is an emergent property of a synaptically coupled network (Del Negro et al. 2002). Although the present study cannot answer the question of whether pacemaker neurons are essential for rhythm generation, this study provides an interesting finding that pacemakers may synchronize multiple network activities through different types of burst mechanisms. However, it must be emphasized that this hypothesis does not negate the critical importance of network mechanisms.

Indeed, the dual-bursting pacemakers described here were cadmium insensitive, although very low (4 μM) concentrations of Cd^{2+} abolish sighs at the population level (Lieske et al. 2000). Our present results are therefore in keeping with the hypothesis that the blockade of fictive sighs by Cd^{2+} results from a disruption of a synaptic mechanism (Lieske et al. 2006a,b) rather than an intrinsic cellular mechanism. In that case, the generation of sighs is likely very sensitive to mechanisms underlying network synchronization.

Our data suggest that postsigh apnea is an expected consequence of pacemakers that trigger activation of an even larger population of neurons than those activated during fictive eupnea. Postsigh apnea results in part from activation of inspiratory neurons to depolarized levels greater than that which occur during eupneic bursts (Lieske et al. 2000). For a network dependent on the activation of burst mechanisms, this additional activation would result in an increased refractory time, causing a delay before the subsequent eupneic burst. Further, the majority of postsigh apnea probably does not result from chemical inhibitory synaptic input to inspiratory neurons immediately following a sigh. Several lines of evidence support these hypotheses. First, most inspiratory neurons activated during eupnea receive additional depolarization during the sigh burst and the currents activated as a result of this depolarization reset the eupneic rhythm, giving rise to apnea following the sigh (Lieske et al. 2000). Second, although inhibitory synaptic inputs appear to contribute to fictive postsigh apnea (Carley et al. 1998) (Fig. 8B), GABAergic and glycinergic inhibition are not necessary for it to occur (Fig. 8B).

The eupneic and sigh rhythms are present even in the absence of sensory feedback. Fictive sighs were generated not only in slices, where they cannot be triggered by reflexes (Lieske et al. 2000), but also in the highly reduced VRG-island, indicating that modulatory and pacemaking influences from outside the VRG region are not essential for generating sighs.

Within the VRG, intracellular recordings confirm an extensive overlap between neurons active during eupnea and sighs (Lieske et al. 2000). However, we identified a previously undescribed population of respiratory neurons active during fictive sighs but not during fictive eupnea. The presence of sigh-only neurons provides further support for the notion that there are at least two populations of VRG neurons that increase their activity during the sigh. These two populations include inspiratory neurons that burst during both eupneic and sigh bursts (Lieske et al. 2000) as well as sigh-only neurons. Both of these populations are recruited during fictive sighs and likely contribute to the characteristic increased amplitude of the sigh burst in VRG population recordings (Lieske et al. 2000). This increase in VRG inspiratory activity may contribute to the enhanced amplitude of sighs, as compared with eupneic breaths.

Sensory input plays a role in sighing because vagotomy or cutting the carotid sinus nerves abolishes sighs for several hours (Cherniack et al. 1981; Glogowska et al. 1972). When they return, sighs occur at a reduced frequency (Cherniack et al. 1981; Marshall and Metcalfe 1988). These data suggest an important role for sensory feedback in modulating sigh drive. A very similar pattern can also be evoked by brief inflation pulses (Cherniack et al. 1981). Thus the central pattern generator for sighs, although capable of functioning independently, appears to be integrated into a complex network including both peripheral feedback and descending inputs from other areas in the intact animal. The present study has contributed to a better understanding of the central component of the sigh by: 1) identifying a set of pacemaker neurons that generate two distinct bursts that respond to modulatory input similarly to the fictive eupneic and sigh activity produced by the network; 2) identifying a set of neurons specifically activated during sighs; and 3) proposing that intrinsic mechanisms could in part explain postsigh apneas.

Acknowledgments

We thank B. Forster for editing the manuscript prior to submission.

GRANTS

This work was supported by National Heart, Lung, and Blood Institute Grants R01-HL-079294 to A. K. Tryba and R01-HL/NS-60120 and HL-68860 to J.-M. Ramirez; a Parker B. Francis Fellowship to A. K. Tryba; and Consejo Nacional de Ciencia y Tecnología de México Grant Conacyt-42870 to F. Peña.

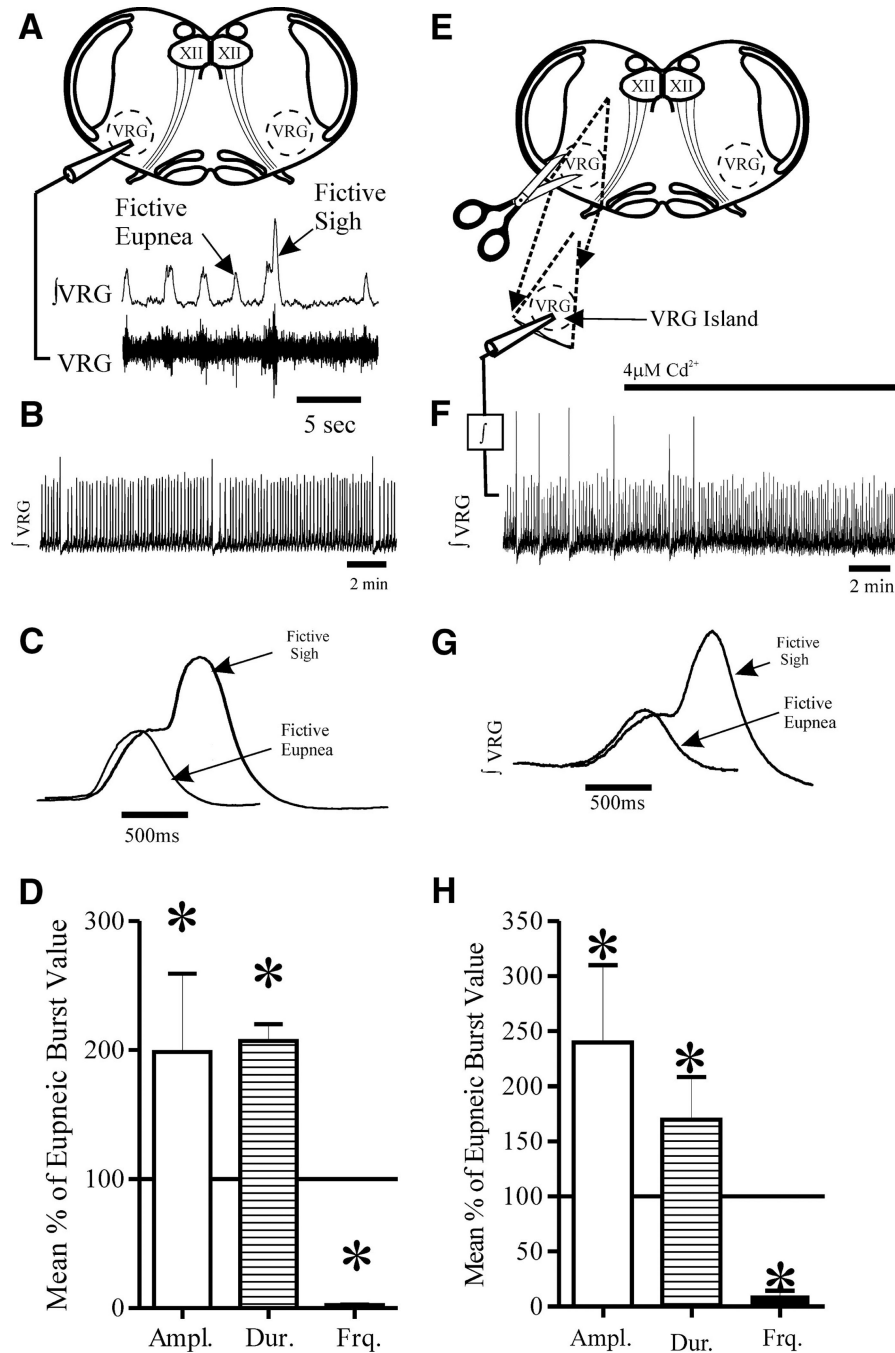
REFERENCES

- Alheid GF, Milsom WK, McCrimmon DR. Pontine influences on breathing: an overview. *Respir Physiol Neurobiol.* 2004; 143:105–114. [PubMed: 15519548]
- Bartos M, Nusbaum MP. Intercircuit control of motor pattern modulation by presynaptic inhibition. *J Neurosci.* 1997; 17:2247–2256. [PubMed: 9065486]
- Buzsáki G, Draguhn A. Neuronal oscillations in cortical networks. *Science.* 2004; 304:1926–1929. [PubMed: 15218136]
- Carley DW, Trbovic Sinisa M, Radulovacki M. Diazepam suppresses sleep apneas in rats. *Am J Respir Crit Care Med.* 1998; 157:917–920. [PubMed: 9517612]
- Cherniack NS, von Euler C, Glogowska M, Homma I. Characteristics and rate of occurrence of spontaneous and provoked augmented breaths. *Acta Physiol Scand.* 1981; 111:349–360. [PubMed: 6797251]
- Chrobak JJ, Buzsáki G. Selective activation of deep layer (V–VI) retrohippocampal cortical neurons during hippocampal sharp waves in the behaving rat. *J Neurosci.* 1994; 14:6160–6170. [PubMed: 7931570]
- Clemens S, Massabuau J-C, Legeay A, Meyrand P, Simmers J. In vivo modulation of interacting central pattern generators in lobster stomatogastric ganglion: influence of feeding and partial pressure of oxygen. *J Neurosci.* 1998; 18:2788–2799. [PubMed: 9502835]

- Csicsvari J, Jamieson B, Wise KD, Buzsáki G. Mechanisms of gamma oscillations in the hippocampus of the behaving rat. *Neuron*. 2003; 37:311–322. [PubMed: 12546825]
- Debarbieux F, Brunton J, Charpak S. Effect of bicuculline on thalamic activity: a direct blockade of I_{AHP} in reticularis neurons. *J Neurophysiol*. 1998; 79:2911–2918. [PubMed: 9636097]
- Del Negro CA, Morgado-Valle C, Feldman JL. Respiratory rhythm: an emergent network property? *Neuron*. 2002; 34:821–830. [PubMed: 12062027]
- Del Negro CA, Morgado-Valle C, Hayes JA, Mackay DD, Pace RW, Crowder EA, Feldman JL. Sodium and calcium current-mediated pacemaker neurons and respiratory rhythm generation. *J Neurosci*. 2005; 25:446–453. [PubMed: 15647488]
- Dickinson PS. Interactions among neural networks for behavior. *Curr Opin Neurobiol*. 1995; 5:792–798. [PubMed: 8805420]
- Elsen FP, Ramirez J-M. Hypoxia reduces the amplitude of voltage dependent calcium currents in the isolated respiratory system of mice. *Soc Neurosci Abstr*. 1997; 27:495.411.
- Elsen FP, Ramirez J-M. Postnatal development differentially affects voltage-activated calcium currents in respiratory rhythmic versus nonrhythmic neurons of the pre-Bötzinger complex. *J Neurophysiol*. 2005; 94:1423–1431. [PubMed: 15888528]
- Feldman JL, Del Negro CA. Looking for inspiration: new perspectives on respiratory rhythm. *Nat Rev Neurosci*. 2006; 7:232–241. [PubMed: 16495944]
- Feldman JL, Smith JC. Cellular mechanisms underlying modulation of breathing pattern in mammals. *Ann NY Acad Sci*. 1989; 563:114–130. [PubMed: 2476055]
- Franco P, Verheulpen D, Valente F, Kelmanson I, de Broca A, Scaillet S, Groswasser J, Kahn A. Autonomic responses to sighs in healthy infants and in victims of sudden infant death. *Sleep Medicine*. 2003; 4:569–577. [PubMed: 14607352]
- Glogowska M, Richardson PS, Widdicombe JG, Winning AJ. The role of the vagus nerves, peripheral chemoreceptors and other afferent pathways in the genesis of augmented breaths in cats and rabbits. *Respir Physiol*. 1972; 16:170–196.
- Goaillard J-M, Schulz DJ, Kilman VL, Marder E. Octopamine modulates the axons of modulatory projection neurons. *J Neurosci*. 2004; 24:7063–7073. [PubMed: 15306640]
- Gray CM, McCormick DA. Chattering cells: superficial pyramidal neurons contributing to the generation of synchronous oscillations in the visual cortex. *Science*. 1996; 274:109–113. [PubMed: 8810245]
- Heinzel HG, Selverston AI. Gastric mill activity in the lobster. III. Effects of proctolin on the isolated central pattern generator. *J Neurophysiol*. 1988; 59:566–585. [PubMed: 3351574]
- Hooper SL, Moulins M. Switching of a neuron from one network to another by sensory-induced changes in membrane properties. *Science*. 1989; 244:1587–1580. [PubMed: 2740903]
- Issa FG, Porostocky S. Effect of sleep on changes in breathing pattern accompanying sigh breaths. *Respir Physiol*. 1993; 93:175–187. [PubMed: 8210757]
- Johnson SM, Koshiya N, Smith JC. Isolation of the kernel for respiratory rhythm generation in a novel preparation: the pre-Bötzinger complex “island”. *J Neurophysiol*. 2001; 85:1772–1776. [PubMed: 11287498]
- Johnson SW, Seutin V. Bicuculline methiodide potentiates NMDA-dependent burst firing in rat dopamine neurons by blocking apamin-sensitive Ca^{2+} -activated K^{+} currents. *Neurosci Lett*. 1997; 231:13–16. [PubMed: 9280156]
- Kay LM. Two species of gamma oscillations in the olfactory bulb: dependence on behavioral state and synaptic interactions. *J Integr Neurosci*. 2003; 2:31–44. [PubMed: 15011275]
- Lieske SP, Ramirez J-M. Pattern-specific synaptic mechanisms in a multi-functional network. II. Intrinsic modulation by metabotropic glutamate receptors. *J Neurophysiol*. 2006a; 95:1334–1344. [PubMed: 16492945]
- Lieske SP, Ramirez J-M. Pattern-specific synaptic mechanisms in a multi-functional network. I. Effects of alterations in synapse strength. *J Neurophysiol*. 2006b; 95:1323–1333. [PubMed: 16492944]
- Lieske SP, Thoby-Brisson M, Telgkamp P, Ramirez J-M. Reconfiguration of the neural network controlling multiple breathing patterns: eupnea, sighs and gasps. *Nat Neurosci*. 2000; 3:600–607. [PubMed: 10816317]

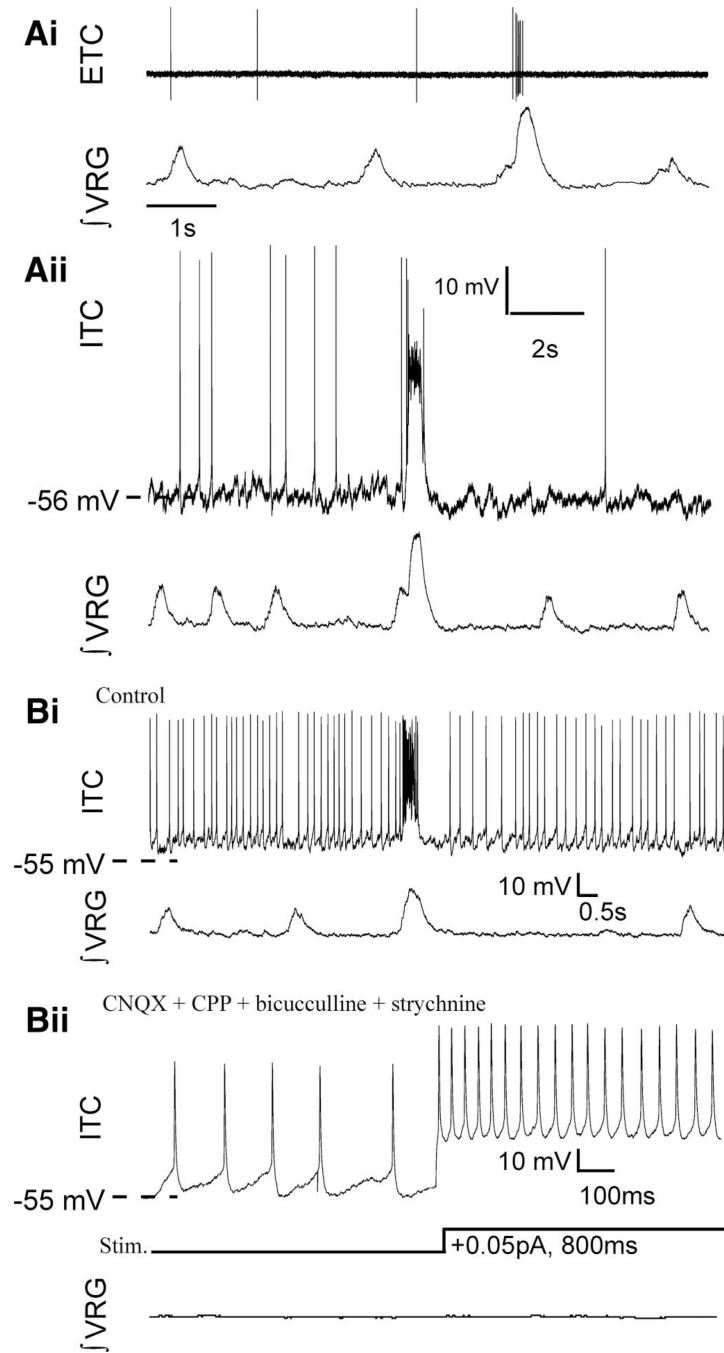
- Marder E, Manor Y, Nadim F, Bartos M, Nusbaum MP. Frequency control of a slow oscillatory network by a fast rhythmic input: pyloric to gastric mill interactions in the crab stomatogastric nervous system. *Ann NY Acad Sci.* 1998; 860:226–238. [PubMed: 9928315]
- Marshall JM, Metcalfe JD. Cardiovascular changes associated with augmented breaths in normoxia and hypoxia in the rat. *J Physiol.* 1988; 400:15–27. [PubMed: 3418526]
- Meyrand P, Simmers J, Moulins M. Construction of a pattern-generating circuit with neurons of different networks. *Nature.* 1991; 351:60–63. [PubMed: 2027383]
- Orem J, Trotter RH. Medullary respiratory neuronal activity during augmented breaths in intact unanesthetized cats. *J Appl Physiol.* 1993; 74:761–769. [PubMed: 8458793]
- Paton JF. The ventral medullary respiratory network of the mature mouse studied in a working heart-brainstem preparation. *J Physiol.* 1996; 493:819–831. [PubMed: 8799902]
- Peña F, Parkis MA, Tryba AK, Ramirez J-M. Differential contribution of pacemaker properties to the generation of respiratory rhythms during normoxia and hypoxia. *Neuron.* 2004; 43:105–117. [PubMed: 15233921]
- Peña F, Ramirez J-M. Endogenous activation of serotonin-2A receptors is required for respiratory rhythm generation in vitro. *J Neurosci.* 2002; 22:11055–11064. [PubMed: 12486201]
- Peña F, Ramirez J-M. Substance P-mediated modulation of pacemaker properties in the mammalian respiratory network. *J Neurosci.* 2004; 24:7549–7556. [PubMed: 15329402]
- Prinz AA, Bucher D, Marder E. Similar network activity from disparate circuit parameters. *Nat Neurosci.* 2004; 7:1345–1352. [PubMed: 15558066]
- Ramirez J-M, Viemari J-C. Determinants of inspiratory activity. *Respir Physiol Neurobiol.* 2005; 147:145–157. [PubMed: 15964786]
- Steriade M. Grouping of brain rhythms in corticothalamic systems. *Neuroscience.* 2006; 137:1087–1106. [PubMed: 16343791]
- Steriade M, McCormick DA, Sejnowski TJ. Thalamocortical oscillations in the sleeping and aroused brain. *Science.* 1993a; 262:679–685. [PubMed: 8235588]
- Steriade M, Nunez A, Amzica F. Intracellular analysis of relations between the slow (<1 Hz) neocortical oscillation and other sleep rhythms of the electroencephalogram. *J Neurosci.* 1993b; 13:3266–3283. [PubMed: 8340807]
- St-John WM, Rudkin AH, Harris MR, Leiter JC, Paton JF. Maintenance of eupnea and gasping following alterations in potassium ion concentration of perfusates of in situ rat preparation. *J Neurosci Methods.* 2005; 142:125–129. [PubMed: 15652625]
- Tabor R, Yaksi E, Weislogel J-M, Friedrich RW. Processing of odor mixtures in the zebrafish olfactory bulb. *J Neurosci.* 2004; 24:6611–6620. [PubMed: 15269273]
- Takeda M, Matsumoto S. Effects of NMDA and non-NMDA receptor antagonists on the medullary inspiratory neuronal activity during spontaneous augmented breaths in anesthetized rats. *Brain Res.* 1998; 781:194–201. [PubMed: 9507124]
- Thoby-Brisson M, Ramirez J-M. Identification of two types of inspiratory pacemaker neurons in the isolated respiratory neural network of mice. *J Neurophysiol.* 2001; 86:104–112. [PubMed: 11431492]
- Thuma JB, Hooper SL. Quantification of gastric mill network effects on a movement-related parameter of pyloric network output in the lobster. *J Neurophysiol.* 2002; 87:2372–2384. [PubMed: 11976375]
- Tryba AK, Peña F, Ramirez J-M. Stabilization of bursting in respiratory pacemaker neurons. *J Neurosci.* 2003; 23:3538–3546. [PubMed: 12716963]
- Tryba AK, Peña F, Ramirez J-M. Gasping activity in vitro: a rhythm dependent on 5-HT_{2A} receptors. *J Neurosci.* 2006; 26:2623–2634. [PubMed: 16525041]
- Tryba AK, Ritzmann RE. Multi-joint coordination during walking and foothold searching in the *Blaberus cockroach*. I. Kinematics and electromyograms. *J Neurophysiol.* 2000; 83:3323–3336. [PubMed: 10848552]
- Viemari J-C, Roux JC, Tryba AK, Saywell V, Burnet H, Peña F, Zanella S, Beventug M, Barthelemy-Requin M, Herzing LB, Moncla A, Mancini J, Ramirez J-M, Villard L, Hilaire G. *Mecp2* deficiency disrupts norepinephrine and respiratory systems in mice. *J Neurosci.* 2005; 25:11521–11530. [PubMed: 16354910]

- Weimann JM, Marder E. Switching neurons are integral members of multiple oscillatory networks. *Curr Biol.* 1994; 4:896–902. [PubMed: 7850423]
- Weimann JM, Meyrand P, Marder E. Neurons that form multiple pattern generators: identification and multiple activity patterns of gastric/pyloric neurons in the crab stomatogastric system. *J Neurophysiol.* 1991; 65:111–122. [PubMed: 1999725]
- Wood DE, Manor Y, Nadim F, Nusbaum MP. Intercircuit control via rhythmic regulation of projection neuron activity. *J Neurosci.* 2004; 24:7455–7463. [PubMed: 15329392]

**FIG. 1.**

The medullary brain slice preparation containing the pre-Bötzinger complex (pre-Böt) generates both fictive eupneic and sigh activity. **A**: diagram of the medullary brain slice that contains the pre-Böt complex within the ventral respiratory group (VRG). The hypoglossal nuclei (XII) are also within the slice. Extracellular population recordings are made from the slice surface (VRG). The integrated trace (\int VRG) is dominated by inspiratory neuron activity as it is in-phase with inspiratory XII motor neuron activation (Tryba et al. 2006). Fictive eupneic bursts and sigh bursts are indicated in the \int VRG trace. **B**: the \int VRG trace shows both fictive eupnea (lower amplitude bursts) and lower frequency fictive sighs (large

amplitude bursts) that are followed by a brief fictive apnea, or cessation of eupneic bursts (Lieske et al. 2000). *C*: averaged fictive eupneic bursts ($n = 16$) and a sigh bursts ($n = 6$) from a single preparation, illustrating that fictive eupnea and biphasic, “eupneic-triggered” sigh bursts, are clearly different in amplitude and duration. *D*: note also that the mean (\pm SD) fictive sigh burst amplitude and duration are larger than fictive eupneic bursts, while sigh burst frequency is lower than fictive eupneic bursts ($n = 14$ slices). *E*: the VRG island preparation was made by cutting away most of the slice and leaving a wedge-shaped piece containing the VRG. *F*: population recordings were made and integrated (\int). The \int VRG island activity always included both fictive eupnea and sighs under control conditions ($n = 4/4$ preparations). Addition of $4 \mu\text{M Cd}^{2+}$ selectively blocked sighs. *G*: an expanded view of averaged \int VRG records from a VRG island preparation shows both fictive eupnea ($n = 13$ averaged from a single preparation) and sighs ($n = 5$ averaged from the same preparation) are similar to those in the more intact slice preparation (*C*); similar results were obtained in $n = 4/4$ preparations). *H*: as was the case in the more intact brain slice (*A*), in the VRG-island preparation, the mean (\pm SD) fictive sigh burst amplitude and duration are larger than fictive eupneic bursts, whereas sigh burst frequency is lower than fictive eupneic bursts ($n = 4$ slices).

**FIG. 2.**

A new class of respiratory neurons are represented here, by “sigh-only” neurons that burst during fictive sighs (not eupnea); interestingly, no “sigh-only” pacemakers have been discovered. *Ai*: extracellular (ETC) recording (*top*) of a “sigh-only” neuron, active during fictive sigh bursts (\int VRG), but not fictive eupneic bursts. *Aii*: subsequent intracellular (ITC) whole cell patch recordings of sigh only neurons revealed they had similar firing patterns during network (\int VRG) activity as when recorded extracellularly (same cell as in *Ai*). *Bi*: a sigh-only neuron that is tonically active between fictive eupneic population burst, but inhibited during fictive eupnea. *Bii*: none of the sigh-only neurons tested was

rhythmically active or showed voltage-dependent bursting properties on depolarizing current injection (bottom traces) following blockade of chemical synaptic transmission, with 6-cyano-7-nitroquinoxaline-2,3-dione (CNQX), (*RS*)-3-(2-carboxypiperazin-4-yl)-propyl-1-phosphonic acid [(*RS*)-CPP, or CPP], bicuculline, and strychnine (same cell as in *Bi*).

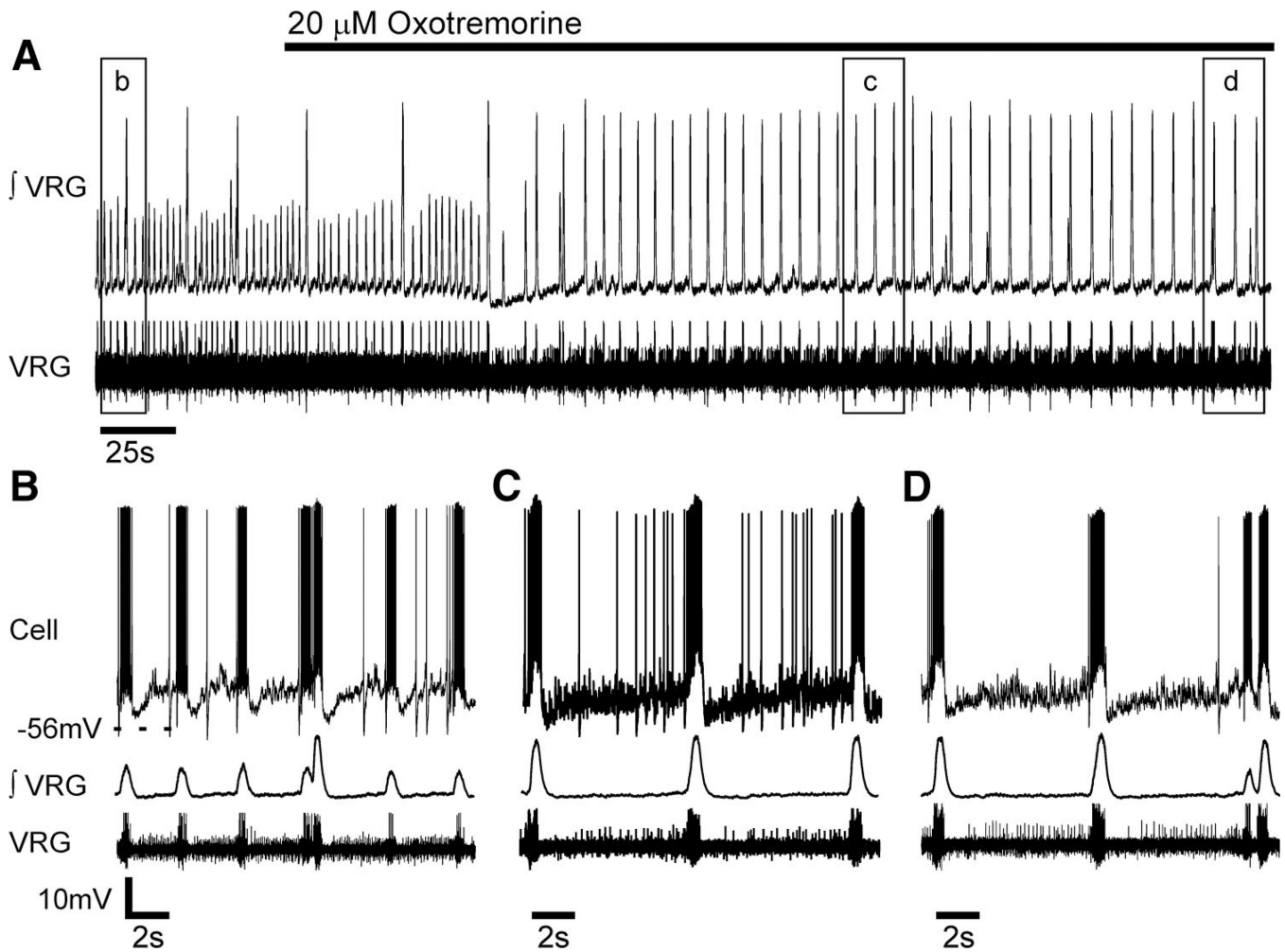
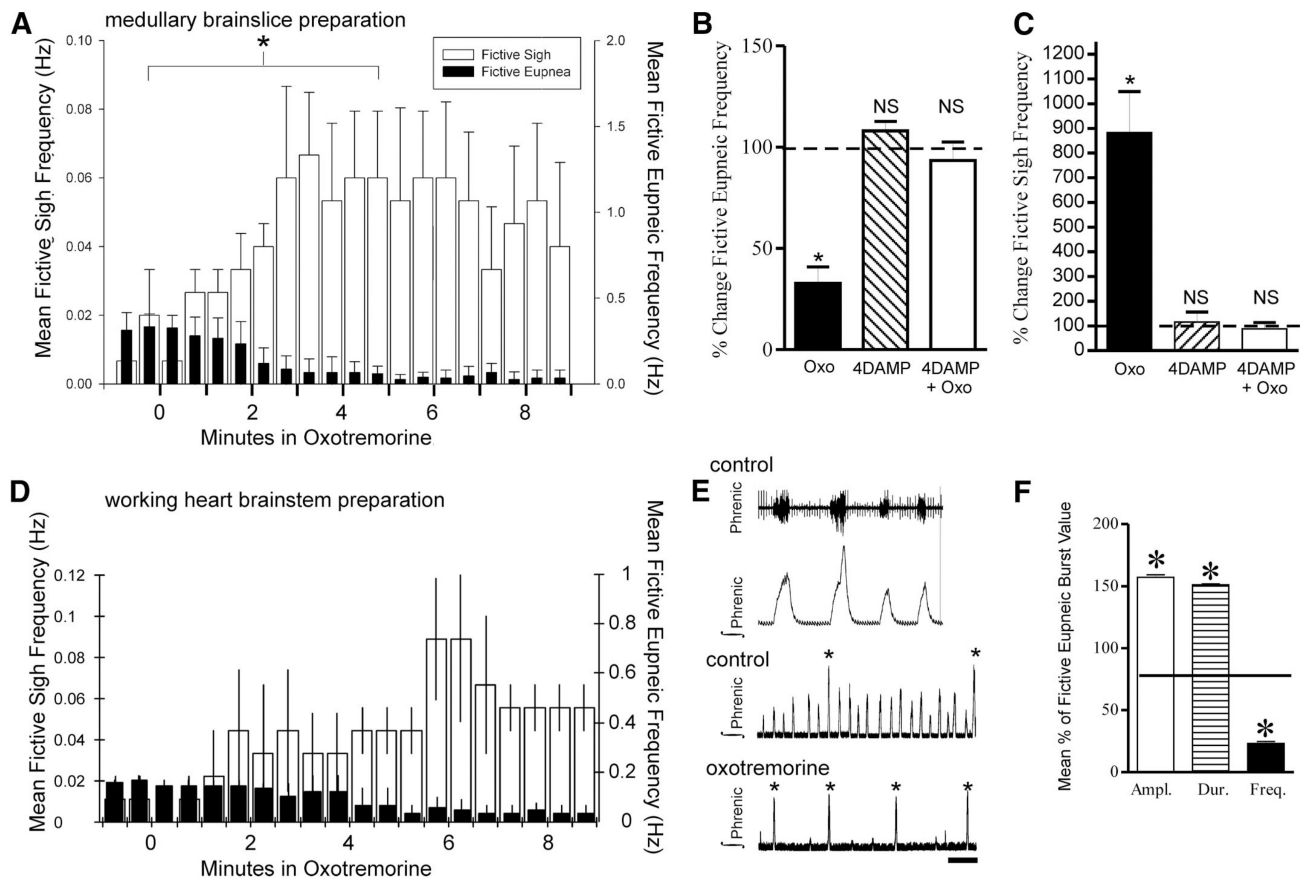


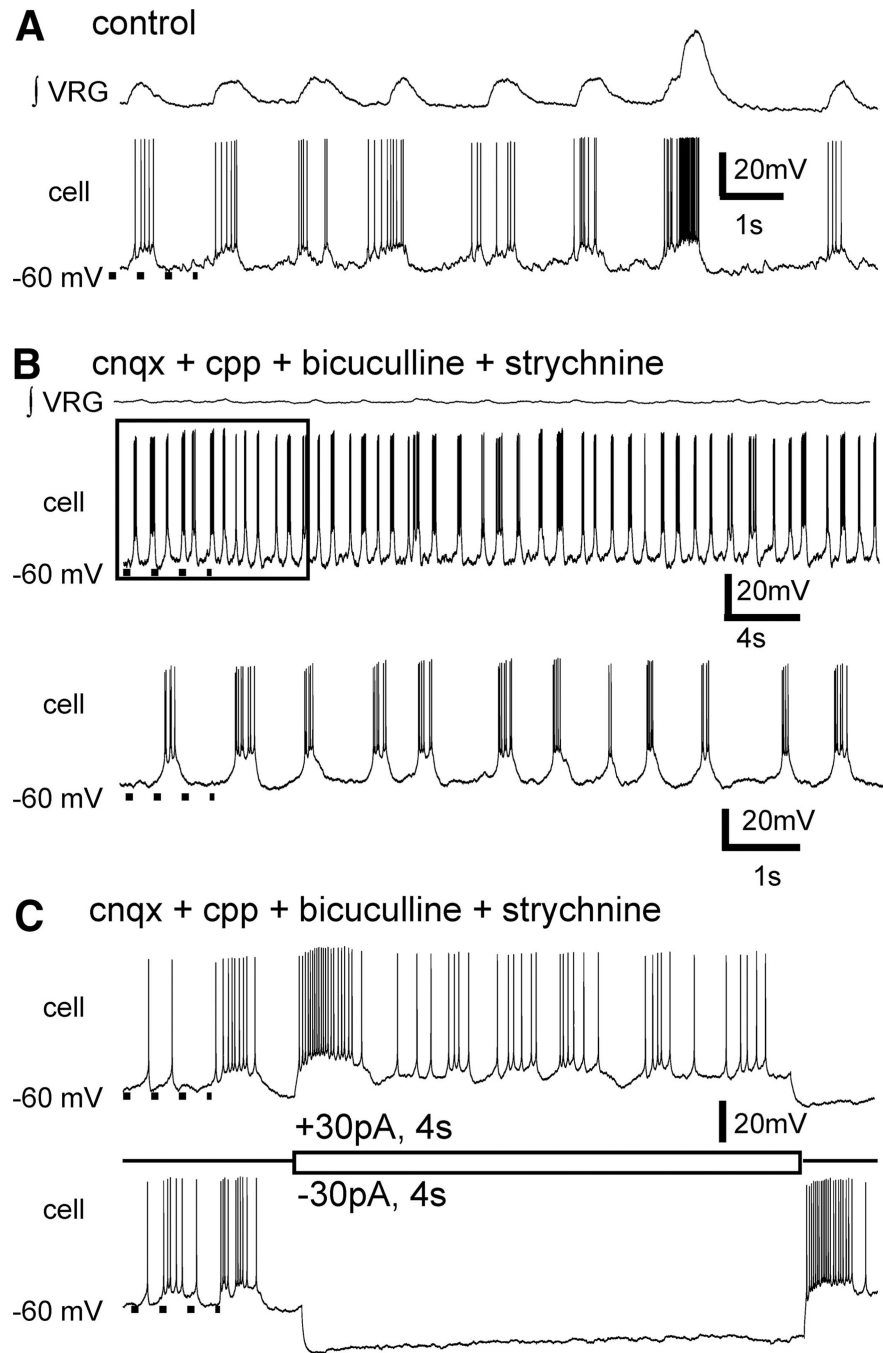
FIG. 3.

Bath-applied oxotremorine modulates the respiratory network population activity (\int VRG) from generating both fictive eupnea and sighs to preferentially generating fictive sigh bursting. *A*: bath-applied oxotremorine ($20 \mu\text{M}$) suppressed *in vitro* fictive eupneic bursts and triggered fictive sighs at an increased frequency (\int VRG, *top*). Note the altered pattern of VRG activity in the raw population record (*bottom*). Boxed areas are expanded below in *B–D* and combined with whole cell current-clamp records (*top*), to reveal that oxotremorine alters cellular and population activity.

**FIG. 4.**

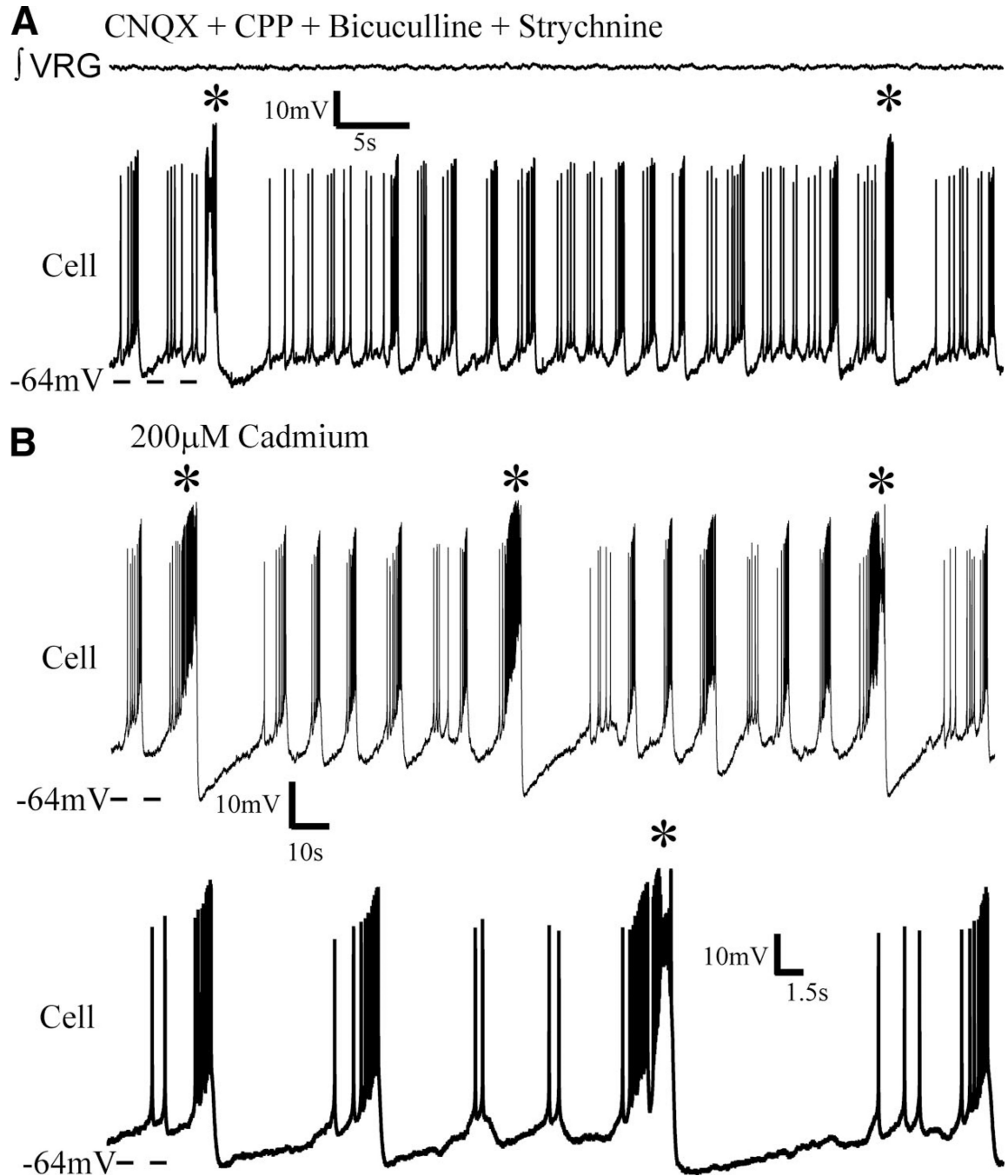
Oxotremorine suppresses fictive eupneic bursts while increasing fictive sigh bursting recorded from the in vitro slice preparation and in situ working heart– brain stem preparation. *A*: \int VRG burst histogram reveals in vitro application of oxotremorine (20 μ M) suppresses eupneic bursting frequency ($P = 0.001$), whereas fictive sigh frequency increases ($P = 0.004$; $n = 10$ slice preparations). For both fictive eupnea and sighs, frequency changes were compared using Wilcoxon signed-rank test at indicated (*) times before ($t = -0.5$ – 0 min) or after ($t = 4.5$ – 5.0 min) adding oxotremorine, when the effect of oxotremorine plateaus (*A*). The effect of oxotremorine application was blocked by 4-DAMP as shown in *B*. Oxotremorine (10 μ M) significantly suppressed fictive eupnea (*B*, $P = 0.001$, Wilcoxon signed-rank test) and enhanced fictive sighing frequency (*C*, $P = 0.004$, Wilcoxon signed-rank test) ($n = 6$ slices, black bars). Bath applying the M3-preferring muscarinic acetylcholine receptor (mAChR) antagonist, 4-DAMP (1 μ M) alone for 10 min had no significant effect on fictive eupneic (*B*, hashed bar) or fictive sigh bursting frequencies (*C*, $n = 6$, hashed bars, $P = 0.18$ eupneic, $P = 0.53$ sighs, Wilcoxon signed-rank test). *B* and *C*: preincubation in 4-DAMP (for 10 min) prevented an expected oxotremorine induced suppression of fictive eupnea or enhanced fictive sigh bursting frequency typically observed following addition of 10 μ M oxotremorine (white bars, $P = 0.52$ eupneic, $P = 0.63$ sigh, Wilcoxon signed-rank test; $n = 4/4$ slices). *D*–*F*: in the in situ working heart– brain stem preparation, oxotremorine also suppresses fictive eupneic bursts, measured at the phrenic nerve, while increasing fictive sigh bursting. *D*: histogram showing oxotremorine (10 μ M) perfused through the working heart– brain stem preparation suppressed fictive eupneic frequency ($P = 0.02$) while fictive sigh bursts increased. ($P = 0.029$) ($n = 4$ preparations, Student's paired t -test). For both fictive eupnea and sighs, frequency changes were

compared using student's *t*-test at before ($t = -0.5-0$ min) or after ($t = 5.5- 6.0$ min) adding oxotremorine, when the effect of oxotremorine was maximal. *E* and *F*: as in vitro, fictive eupnea and sighs are distinguishable in the in situ preparation, as fictive eupneic bursts are smaller in amplitude, shorter in duration, and occur at a faster frequency than eupneic bursts. Asterisks in *E* denote fictive sigh bursts.

**FIG. 5.**

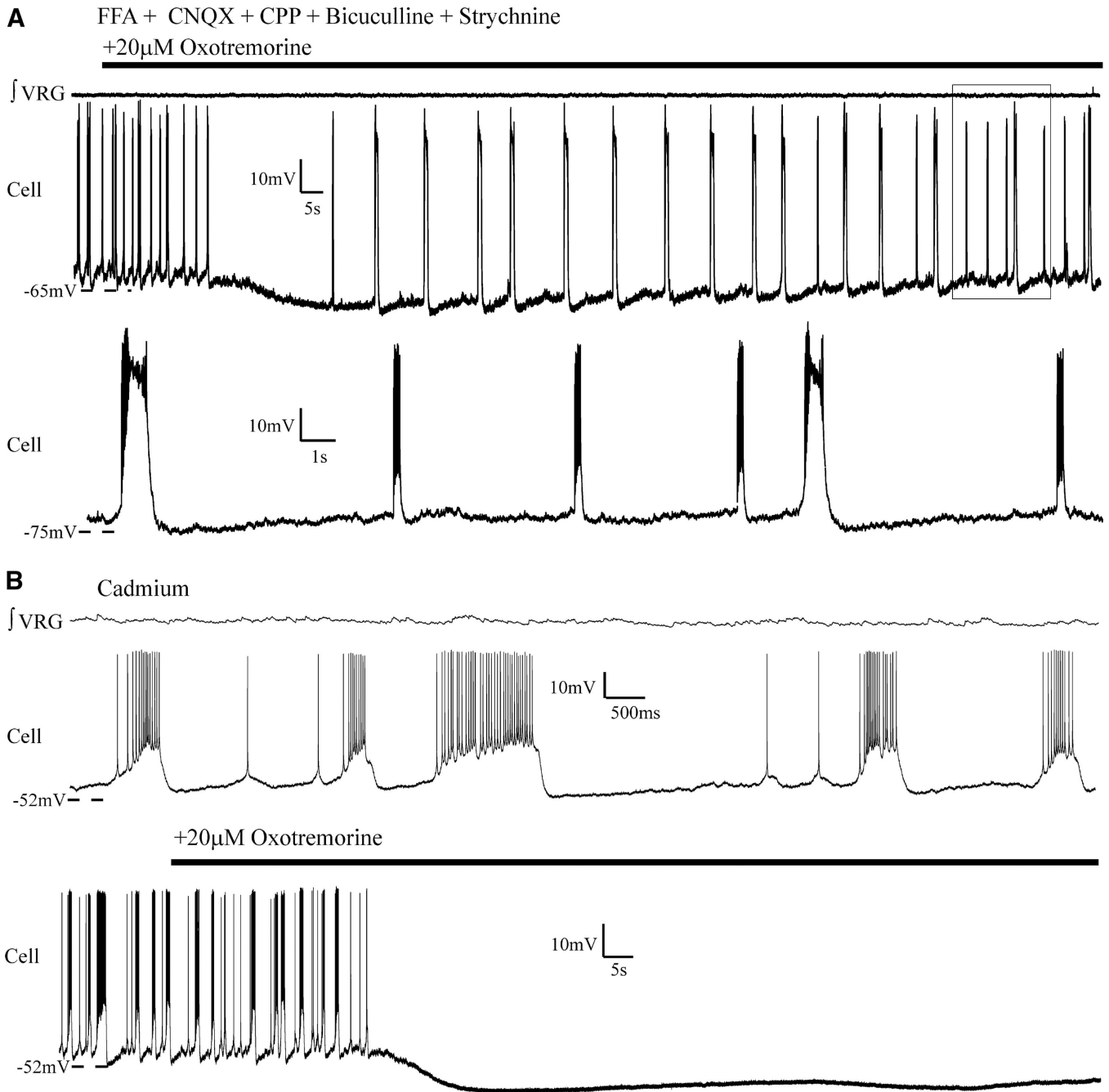
A subset of inspiratory neurons have endogenous voltage-dependent pacemaker bursting properties. *A*: inspiratory neurons burst in-phase with fictive eupneic and sigh VRG activities and, as in this case, *(B)* a subset of inspiratory neurons continue to generate voltage-dependent bursting properties, following blockade of ionotropic receptors with CNQX, CPP, bicuculline, and strychnine and loss of network (\int VRG) rhythmic bursting. Typically, the bursting properties of synaptically isolated inspiratory pacemakers does not include fictive sigh-like bursts (*top*). *Bottom*: an expanded view of boxed area shown in the

top panel. C: inspiratory pacemakers retain voltage-dependent bursting properties following synaptic isolation.

**FIG. 6.**

Following isolation from ionotropic chemical transmission, some inspiratory pacemakers continue to generate two different types of bursts at two different frequencies. *A*: a subset of previously undescribed isolated pacemakers generate both shorter, higher frequency bursts and longer bursts at a lower frequency [starred (*) bursts]. Synaptic transmission was blocked with CNQX, CPP, bicuculline and strychnine, yet this neuron continued to generate both faster bursts and larger slower bursts (starred), even following (*B*) subsequent addition of cadmium, that is a nonspecific blocker of calcium mediated synaptic transmission. Note

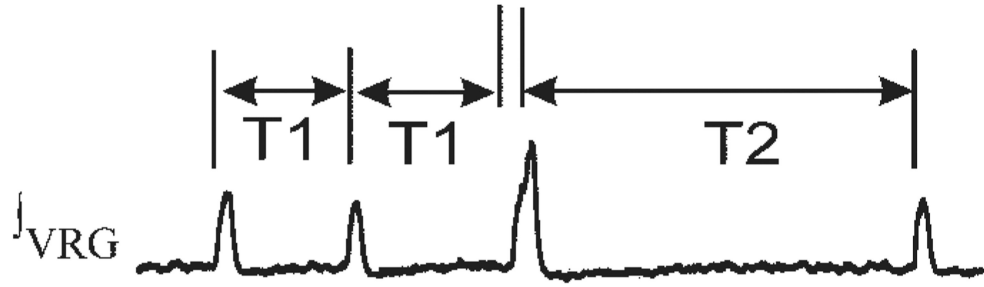
(*bottom trace in B*) the starred, lower frequency, longer duration bursts are characteristically sigh-like, in that it is biphasic and followed by a phase-reset of shorter, faster bursts.

**FIG. 7.**

Application of oxotremorine to a subset of synaptically isolated pacemakers suppressed faster eupneic-like burst activity and triggered large sigh-like bursting activity. *A*: as was seen at the network level, oxotremorine application (20 μ M) also triggered sigh-like bursts and suppressed shorter eupneic-like bursting activity in some isolated pacemakers. Shorter eupneic bursts returned with continued application (boxed area). *Bottom trace* is expansion of area boxed in *top trace*. Note that sigh-like bursting activity resulted in a phase reset of the eupneic-like bursts. Ten minutes prior to adding oxotremorine, flufenamic acid (FFA, 500 μ M) was added; FFA-insensitive pacemakers are typically cadmium insensitive [as previously shown (Peña et al. 2004)]. *B*: not all cadmium-insensitive pacemakers that

intrinsically generated differential bursting patterns, following synaptic isolation (*top traces*), continued to generate bursting with subsequent oxotremorine application (*bottom traces*, $n = 2$).

A Time (T) points for measuring delay in cycle period delay following sigh



B Delay in Fictive Eupnea Cycle Period Following Sigh in Control vs After Blockade of Inhibition

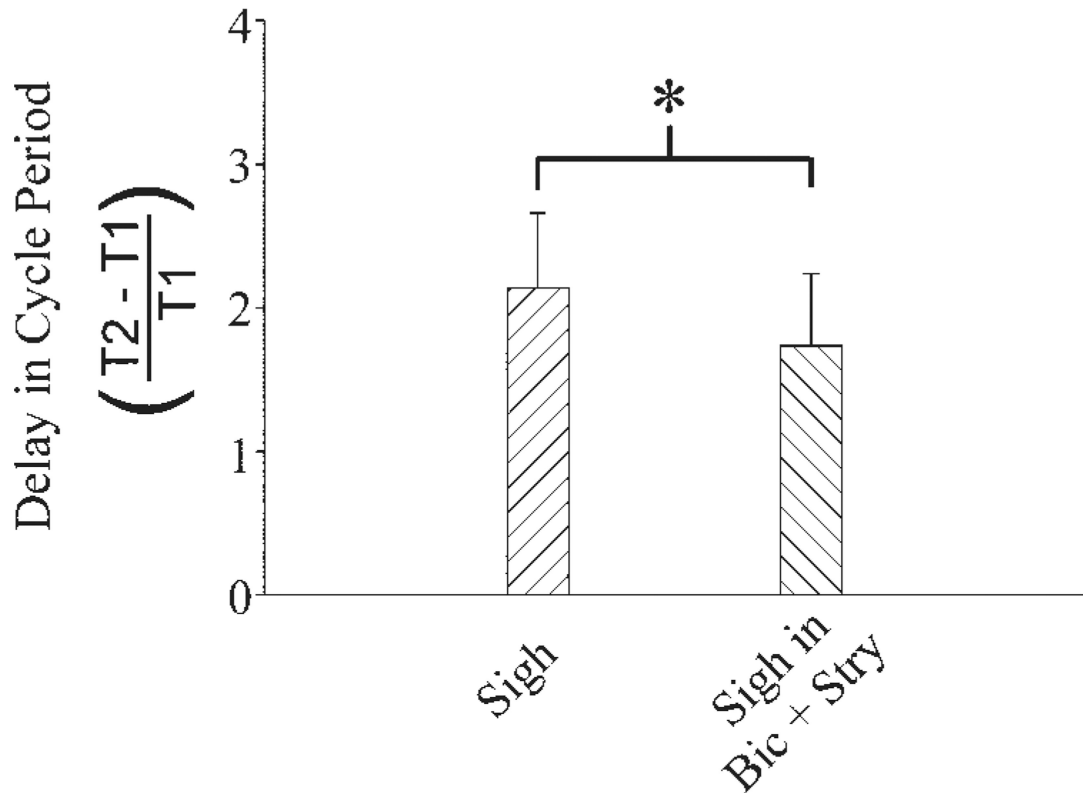


FIG. 8. Intrinsic membrane properties may explain postsigh apnea. *A*: diagram of time reference points used for definition of delay in fictive eupneic burst period following a fictive sigh burst. *B*: mean delay (\pm SD bars) in fictive eupneic cycle period following a sigh burst in control saline (sigh) or following bath application of bicuculline (20 μ M) and strychnine (1 μ M) (sigh in Bic + Stry). Cycle periods were determined from population (f VRG) records from $n = 4$ preparations.